Published in final edited form as:

Physiol Res. 2015 ; 64(6): 857–873.

Inhibition of soluble epoxide hydrolase does not improve the course of congestive heart failure and the development of renal dysfunction in rats with volume overload induced by aorto-caval fistula

Luděk Červenka[1,2,*], **Vojtěch Melenovský**[3,*], **Zuzana Husková**[2], **Alexandra Sporková**[2], **Marcela Bürgelová**[2], **Petra Škaroupková**[2], **Sung Hee Hwang**[4], **Bruce D. Hammock**[4], **John D. Imig**[5], and **Janusz Sadowski**[6]

[1] Department of Pathophysiology, 2nd Faculty of Medicine, Charles University, Prague, Czech Republic [2] Center for Experimental Medicine, Institute for Clinical and Experimental Medicine, Prague, Czech Republic [3] Department of Cardiology, Institute for Clinical and Experimental Medicine, Prague, Czech Republic [4] Department of Entomology and UCD Comprehensive Cancer Center, University of California, Davis, One Shields Avenue, Davis, California 95616-8584, USA [5] Department of Pharmacology and Toxicology, Medical College of Wisconsin, Wisconsin, USA [6] Department of Renal and Body Fluid Physiology, M. Mossakowski Medical Research Centre, Polish Academy of Science, Warsaw, Poland

Abstract

The detailed mechanisms determining the course of congestive heart failure (CHF) and associated renal dysfunction remain unclear. In a volume overload model of CHF induced by creation of aorto-caval fistula (ACF) in Hannover Sprague-Dawley (HanSD) rats we explored the putative pathogenetic contribution of epoxyeicosatrienoic acids (EETs), active products of CYP-450 dependent epoxygenase pathway of arachidonic acid metabolism, and compared it with the role of the renin-angiotensin system (RAS). Chronic treatment with *cis*-4-[4-(3-adamantan-1-yl-ureido) cyclohexyloxy]benzoic acid (*c*-AUCB, 3 mg/L in drinking water), an inhibitor of soluble epoxide hydrolase (sEH) which normally degrades EETs, increased intrarenal and myocardial EETs to levels observed in sham-operated HanSD rats, but did not improve the survival or renal function impairment. In contrast, chronic angiotensin-converting enzyme inhibition (ACEi, trandolapril, 6 mg/L in drinking water) increased renal blood flow, fractional sodium excretion and markedly improved survival, without affecting left ventricular structure and performance. Hence, renal dysfunction rather than cardiac remodeling determines long-term mortality in advanced stage of CHF due to volume overload. Strong protective actions of ACEi were associated with suppression of the vasoconstrictor/sodium retaining axis and activation of vasodilatory/natriuretic axis of the renin-angiotensin system in the circulating blood and kidney tissue.

Author for correspondence: Luděk Červenka, M.D., PhD., Department of Pathophysiology, 2nd Faculty of Medicine, Charles University, Prague, Czech Republic., Phone: +420 2 57296200, luce@medicon.cz.

*L.Č. and V.M. should each be considered as the first author.

DISCLOSURE

Authors declare no potential conflict of interest.

Keywords

congestive heart failure; aorto-caval fistula; renin-angiotensin system; epoxyeicosatrienoic acids; soluble epoxide hydrolase

Introduction

Chronic heart failure (CHF) is a major public health problem, with a prevalence of more than 5.8 million in the United States and with steadily increasing prevalence worldwide. In Europe, CHF affects currently almost 4% of the adult population (Dickstein *et al.* 2008, Roger 2013). Despite the recent therapeutical advances, the prognosis of CHF still remains poor (Dickstein *et al.* 2008, Katz 2003, Roger 2013). Development of renal dysfunction in the context of CHF due to impairment of renal hemodynamics and sodium excretion (Braam *et al.* 2014, Giamouzis *et al.* 2013) is associated with markedly increased risk of death (Ronco C *et al.* 2008). Therefore, exploration of pathophysiological mechanisms and examination of novel therapeutical approaches targeting renal dysfunction in CHF are needed to improve prognosis.

Vast evidence indicates that epoxyeicosatrienoic acids (EETs), cytochrome P-450 (CYP)-dependent metabolites of arachidonic acid, are involved in the regulation of cardiovascular and renal function (Elmarakby 2012, Imig 2012). EETs are biologically unstable (Elmarakby 2012, Imig 2012), which limits their direct therapeutical potential. However, tissue EET bioavailability can be increased by blocking soluble epoxide hydrolase (sEH), an enzyme responsible for degradation of EETs to biologically inactive dihydroxyeicosatrienoic acids (DHETEs) (Elmarakby 2012, Honetschlagerová *et al.* 2011, Imig 2012, Kopkan *et al.* 2013, Kujal *et al.* 2014, Neckář *et al.* 2012, Sporková *et al.* 2011). Increasing tissue EETs levels by preventing their degradation to DHETEs was shown to have antihypertensive effect related to EETs-mediated vasodilation and to direct influence on renal tubular transport of sodium (Elmarakby 2012, Honetschlagerová *et al.* 2011, Imig 2012, Kopkan *et al.* 2012). Moreover, it has been shown that experimental alteration of the gene encoding sEH (*Ephx2*) facilitates the progression from hypertension and cardiac hypertrophy to CHF, and *Ephx2* locus was identified as a CHF susceptibility gene in a rat model of hypertension and CHF (Monti *et al.* 2008). Furthermore, many studies indicate a protective action of EETs against ischemia/reperfusion (I/R) injury of the heart (Imig 2012, Neckář *et al.* 2012), and an acceleration of cardiac remodeling in chronic kidney disease (CKD) (Zhang *et al.* 2013). It has also been shown that augmentation of EETs' bioavailability by sEH inhibition improved left ventricular (LV) diastolic and systolic function in ischemic model of CHF (Li *et al.* 2009, Merabet *et al.* 2012). Finally, a recent study has demonstrated that chronic sEH inhibition substantially attenuated the progression of CKD in Ren-2 transgenic rats (a unique well-defined monogenetic model of angiotensin II (ANG II)-dependent hypertension) subjected to 5/6 renal mass reduction (5/6 NX) (Kujal *et al.* 2014).

Taken together, these findings suggest that sEH inhibitors may present a new class of drugs for treatment of cardiovascular diseases, in particular of CHF. However, no evidence is available to indicate that chronic sEH inhibition results in a prolongation of life in

individuals with advanced CHF associated with evident renal dysfunction. The rat with CHF induced by aorto-caval fistula (ACF) presents a well-defined model of chronic heart failure due to volume overload, characterized by activation of the renin-angiotensin system (RAS), congestion and impairment of renal function; the model has many features in common with untreated human CHF (Abassi *et al.* 2011, Benes *et al.* 2011, Benes Jr. *et al.* 2011, Brower *et al.* 1996, Cohen-Segev *et al.* 2014, Garcia and Diebold 1990, Hutchinson *et al.* 2011, Lear *et al.* 1997, Melenovsky *et al.* 2011, Melenovsky *et al.* 2012, Oliver-Dussalut *et al.* 2010, Petrak *et al.* 2011, Pieruzzi *et al.* 1995, Ruzicka *et al.* 1993, Yang *et al.* 1993, Wang *et al.* 2003).

In an attempt to address the issues regarding pathogenesis of renal dysfunction in CHF, we aimed here to evaluate the effects of chronic treatment with an sEH inhibitor, *cis*-4-[4-(3-adamantan-1-yl-ureido) cyclohexyloxy]benzoic acid (*c*-AUCB), on the mortality and morbidity indices and on renal function in male, normotensive Hannover Sprague-Dawley (HanSD) rats with ACF-induced CHF. In order to further elucidate the possible beneficial effects of chronic sEH inhibition on the course of ACF-induced CHF, the cardiac structure and function were determined by echocardiography and invasive pressure-volume analysis of the left ventricle, respectively. Finally, to gain a more detailed insight in the possible role of interactions of CYP-derived metabolites with RAS in the pathophysiology of CHF-related renal dysfunction, we determined plasma, heart and renal concentrations of EETs, DHETEs, 20-hydroxyeicosatrienoic acid (20-HETE), ANG II and angiotensin-1-7 (ANG 1-7) in untreated and *c*-AUCB-treated sham-operated and ACF HanSD rats. In addition, kidney and heart tissue protein expressions of CYP2C3, one of the major enzymes responsible for EETs formation, and of sEH, the enzyme responsible for degradation of EETs, were determined.

Materials and Methods

Animals

All HanSD rats used in the present study were bred at the Center for Experimental Medicine from stock animals supplied from Max Delbrück Center for Molecular Medicine, Berlin (we acknowledge the generous gift of Drs. Bader and Ganten). Animals were fed a standard rat chow containing 0.4% sodium chloride (SEMED, Prague, Czech Republic), with free access to tap water throughout the whole experimental protocol. All the animals used in the study were housed in facilities accredited by the Czech Association of Laboratory Animal Care. The studies were performed in accordance with guidelines and practices established by the Animal Care and Use Committee of the Institute for Clinical and Experimental Medicine, Prague, and of the 2nd Faculty of Medicine, Charles University, Prague, which accord with the European Convention on Animal Protection and Guidelines on Research Animal Use.

CHF model and chronic treatments

CHF was induced by volume overload which results from placement of ACF, using a needle technique (18- gauge needle − diameter 1.2 mm) as originally described by Garcia and Diebold (Garcia and Diebold 1990) and employed and validated by many investigators including our own group (Abassi *et al.* 2011, Benes *et al.* 2011a, Benes Jr. *et al.* 2011, Brower *et al.* 1996, Garcia and Diebold 1990, Hutchinson *et al.* 2011, Lear *et al.* 1997,

Melenovsky *et al.* 2011, Melenovsky *et al.* 2012, Oliver-Dussalut *et al.* 2010, Petrak *et al.* 2011, Pieruzzi *et al.* 1995, Ruzicka *et al.* 1993, Yang *et al.* 1993, Wang *et al.* 2003). Sham-operated rats underwent a similar procedure but without creating ACF. *c*-AUCB, the sEH inhibitor (sEHi) was synthesized by S.H.H. and B.D.H in their laboratory by methods described and validated previously (Hwang *et al.* 2007). *c*-AUCB was prepared freshly and given in drinking water at 3 mg/L. The appropriate amount of *c*-AUCB was dissolved with gentle warming in polyethyleneglycol and added with rapid stirring to warm drinking water to give a 0.1 % aqueous solution of polyethylenglycol (Hwang *et al.* 2007). The dose of *c*-AUCB was selected based on our recent studies where it elicited substantial increases in tissue concentration of EETs without altering RAS activity (Kujal *et al.* 2014). We chose the *c*-AUCB dose that blocks sEH activity without altering plasma and tissue ANG II levels with an intention to separate and evaluate the effect of EETs elevation alone on the course of ACF-induced CHF. Since therapeutic regimes involving inhibition of RAS are common or even standard in the therapy of CHF (Ichikawa *et al.* 1984, Katz 2003, Pfeffer *et al.* 1983, Pfeffer *et al.* 1995, Roger 2013, Schroten *et al.* 2012), we employed also the treatment with ACEi to compare the effects with those obtained in the *c*-AUCB-treated groups. Trandolapril (6 mg/L in drinking water; Gopten; Abbot, Prague, Czech Republic), was used to inhibit ACE because in our previous studies and here in preliminary experiments we demonstrated that at this dose the drug provided maximal blockade of RAS and was well tolerated both by rats with ACF-induced CHF and by sham-operated animals (Kujal *et al.* 2014).

Experimental design

Series 1: Assessment of RAS and CYP metabolites in the early phase after ACF-induced CHF—The aim of this series of experiments was to evaluate the degree of activation of the two axes of the RAS: the vasoconstrictor ACE/ANG II axis, and the vasodilator ACE type 2 (ACE2)/ANG 1-7 axis, together with determination of the rate of synthesis along the two CYP-dependent pathways, those of epoxygenase and ω-hydroxylase. Male HanSD rats aged 9 weeks were divided into two experimental groups (the follow-up period was 10 weeks):

1. Sham-operated HanSD rats + vehicle (water) treatment (n = 11)
2. ACF HanSD rats + water treatment (n = 12)

a) Effects of ACF induction on plasma and kidney ANG II and ANG 1-7 concentrations: Since it is now well recognized that ANG II and ANG 1-7 concentrations in anesthetized animals are higher than those obtained from decapitated conscious rats, at the end of experiment plasma and tissue ANG II levels were measured by radioimmuassay. This approach enabled us also to compare the present results with those from our earlier studies of the role of the RAS in the pathophysiology of various cardiovascular diseases (Burgelova *et al.* 2009, Červenka *et al.* in press, Honetschlagerová *et al.* 2011, Husková *et al.* 2010).

b) Effects of ACF induction on tissue concentrations of EETs and DHETEs, and Western blot analysis of protein expression of CYP enzymes: The levels of EETs and DHETEs in the kidney cortex and LV tissue were measured. The samples were extracted, the

extracts were separated by reverse-phase high performance liquid chromatography and analysed by negative-mode electrospray ionization and tandem mass spectroscopy as described previously (Honetschlagerová *et al.* 2011, Neckář *et al.* 2012). Specifically, 8,9-EETs; 11,12-EETs and 14,15-EETs were measured separately and then pooled and presented jointly. These metabolites are the most active products formed in the CYP epoxygenase pathway (Imig 2012). The EETs/DHETES ratio was calculated from total concentrations of EETs and of DHETEs. Western blot analysis of protein expression of CYP2C23, the enzyme that is predominantly responsible for the formation of EETs, and of sEH, the enzyme responsible for the conversion of EETs to DHETEs, were performed as described previously (Kopkan *et al.* 2012, Neckář *et al.* 2012, Sporková *et al.* 2011), with levels normalized against ß-actin. In addition, 20-HETE and protein expression for CYP4A, the enzyme responsible for the formation of 20-HETE, were analysed in the renal and LV tissues as described previously (Kopkan *et al.* 2012, Neckář *et al.* 2012).

Series 2: Effects of sEH and ACE inhibition on the survival rate and signs of CHF—Male HanSD rats of the same age as in series 1 (9 weeks) were derived from several litters randomly assigned to experimental groups, to make sure that animals from a single litter did not prevail in any group. Animals underwent either sham-operation or ACF creation as described above (on the week labeled as −10) and were left without treatment for 10 weeks. Previous studies have shown that 10 weeks after ACF operation cardiac remodeling and renal functional characteristics typical for CHF become apparent. At that time, the rats are at the stage of compensated CHF and still exhibit 100% survival (Melenovský *et al.* 2012). At this time point (week 0) the rats were divided into the following experimental groups:

1. Sham-operated HanSD rats + water (initial n = 10)
2. ACF HanSD rats + water (initial n = 32)
3. ACF HanSD rats + sEHi (initial n = 28)
4. ACF HanSD rats + ACEi (initial n = 27)

The follow-up period was 40 weeks. The rats were inspected daily and body weight (BW) was determined three times per week. In addition, always the same experienced technician (PŠ) monitored animals for presence of CHF symptoms using a scoring system that was developed and verified previously (Melenovský *et al.* 2012). Briefly, each animal was scored with respect to five features of rat CHF: a) presence of raised fur (piloerection), b) diminished activity (lethargy), c) peripheral cyanosis, d) rapid or labored breathing (dyspnea) and e) abdominal swelling (ascites). Each symptom was scored on the scale from 0 to 3 points and a CHF score was calculated for each animal as a sum of individual points.

Series 3: Effects of sEH and ACE inhibition on ANG II, ANG 1-7, EETs, DHETEs and 20-HETE concentration—Animals were prepared as described in series 2 and on week 0 the pharmacological treatment was initiated for a period of 10 weeks. At the end of experiment (on week +10) the rats were killed by decapitation and plasma and kidney ANG II, ANG 1-7, EETs, DHETEs and 20-HETE were measured as described for series 1. The following experimental groups were examined:

1. Sham-operated HanSD rats + water (n = 8)
2. Sham-operated HanSD rats + sEHi (n = 8)
3. Sham-operated HanSD rats + ACEi (n = 7)
4. ACF HanSD rats + water (n = 9)
5. ACF HanSD rats + sEHi (n = 9)
6. ACF HanSD rats + ACEi (n = 9)

Series 4: Effects of sEH and ACE inhibition on renal hemodynamics and excretory function—The following experimental groups exposed to the same protocol as animals in series 3 were examined:

1. Sham-operated HanSD rats + water (n = 7)
2. Sham-operated HanSD rats + sEHi (n = 7)
3. Sham-operated HanSD rats + ACEi (n = 8)
4. ACF HanSD rats + water (n = 12)
5. ACF HanSD rats + sEHi (n = 11)
6. ACF HanSD rats + ACEi (n = 10)

At the end of the experimental protocol (on week +10), the rats were anesthetized and acute clearance experiments were performed as described in detail in our previous studies, to determine renal hemodynamics and excretory parameters (Honetschlagerová *et al.* 2011, Sporková *et al.* 2011).

Series 5: Effects of sEH and ACE inhibition on basal cardiac function parameters assessed by echocardiography and by pressure-volume analysis —In this series the following groups, subjected to the same protocol as animals in series 3, were studied.

1. Sham-operated HanSD rats + water (n = 8)
2. Sham-operated HanSD rats + sEHi (n = 8)
3. Sham-operated HanSD rats + ACEi (n = 9)
4. ACF HanSD rats + water (n = 10)
5. ACF HanSD rats + sEHi (n = 10)
6. ACF HanSD rats + ACEi (n = 10)

At the end of the experimental protocol, animals were anesthetized by intraperitoneal (i.p.) administration of ketamine/midazolam combination (50 mg and 5 mg/kg of body weight, respectively) and echocardiography was performed as described in our recent studies (Benes *et al.* 2012, Neckář *et al.* 2012). Subsequently, rats were intubated with a plastic cannula, relaxed with pancuronium (Pavulon, 0.16.mg/kg) and artificially ventilated (rodent ventilator Ugo Basile, Italy). LV function was invasively assessed by 2F Pressure-Volume (P-V)

micromanometry catheter (Millar Instruments) introduced into the LV cavity via the right carotid artery after previous vagal blockade (atropin 0.10 mg/kg) (Pacher *et al*. 2008). Volume signal was calibrated by end-diastolic and and-systolic volume obtained shortly before invasive recordings. Data were acquired using an 8-channel Power lab recorder and were analyzed by Labchart Pro software (ADinstruments, Australia).

Statistical analysis

Statistical analysis of the data was performed using Graph-Pad Prism software (Graph Pad Software, San Diego, California, USA). Analysis of variance (ANOVA) for repeated measurements, followed by Student-Newman-Keuls test, was performed for analysis within groups (e.g. survival rate). Statistical comparison of other results was made by Student's *t*-test, Wilcoxon's signed-rank test for unpaired data or one-way ANOVA when appropriate. Unless otherwise indicated, values are expressed as mean ± S.E.M. A p value less than 0.05 was considered statistically significant.

Results

Series 1: Assessment of RAS and CYP metabolites in the early phase after ACF-induced CHF

As shown in Figure 1A and 1B, 10 weeks after induction of ACF (i.e. on week 0) plasma and kidney ANG II levels were significantly higher in untreated ACF HanSD rats than in sham-operated HanSD rats. Similarly, plasma and kidney ANG 1-7 concentrations were significantly higher in untreated ACF HanSD rats than in sham-operated HanSD rats (Figures 1C and 1D).

As shown in Figure 2A, the intrarenal availability of biologically active epoxygenase metabolites, expressed as the EETs/DHETEs ratio, was significantly lower in ACF HanSD rats than in sham-operated HanSD rats. Densitometric analysis revealed no significant differences in CYP2C3 protein expression in the renal cortex between ACF HanSD rats and sham-operated HanSD rats (data normalized against ß-actin, Figure 2B). In contrast, sEH protein expression was significantly higher in ACF HanSD rats than in sham-operated HanSD rats (Figure 2C). Figures 2D, 2E and 2F show that LV myocardial tissue exhibits a similar pattern, i.e. lower availability of epoxygenase metabolites, no significant change in CYP2C3 protein expression, and significantly higher sEH protein expression in ACF HanSD rats than observed in sham-operated HanSD rats.

There were no significant differences in the renal and LV myocardial tissue availability of biologically active ω-hydroxylase metabolites, such as 20-HETE, and CYP4A protein expression between ACF HanSD rats and sham-operated HanSD rats (data not shown).

Series 2: Effects of sEH inhibition on the survival rate and signs of CHF

All sham-operated HanSD rats survived until the end of the experiment. As shown in Figure 3A, untreated ACF HanSD rats began to die by week 10 (i.e. 20 weeks after induction of ACF) with a final survival rate of 43 %. Treatment with sEHi did not improve survival rate in ACF HanSD rats as compared with untreated ACF HanSD rats. In contrast, treatment with

ACEi dramatically improved survival rate, to 95%, which was not significantly different from that in sham-operated HanSD rats.

As shown in Figure 3B, the average BW curves were almost identical in sham-operated HanSD rats, untreated ACF HanSD rats and ACF HanSD rats treated with sEHi. Beginning from the week 16 of treatment with ACEi, ACF HanSD rats showed significantly lower BW than that recorded in sham-operated HanSD rats, untreated ACF HanSD rats and ACF HanSD rats treated with sEHi.

As shown in Figure 3C, four weeks before death the CHF score in our ACF animals exceeded the threshold for the CHF established previously (Melenovský *et al.* 2012), and then progressively increased, reaching the maximum two weeks before death. There were no significant differences in this parameter in any of ACF groups and CHF score in sham-operated rats was close to zero throughout the experiment.

Series 3: Effects of sEH and ACE inhibition on ANG II, ANG 1-7, EETs, DHETEs and 20-HETE concentrations

As shown in Figures 4A and 4C, neither sEHi nor ACEi treatment altered plasma ANG II or ANG 1-7 levels in sham-operated rats. However, ACEi (but not sEHi) significantly decreased kidney ANG II and increased kidney ANG 1-7 concentrations in these rats (Figures 4B and 4D). Treatment with sEHi did not modify kidney ANG II concentrations and plasma and kidney ANG 1-7 levels in ACF HanSD rats. In contrast, treatment with ACEi markedly reduced plasma and kidney ANG II levels and significantly increased plasma and kidney ANG 1-7 concentrations in ACF + ACEi group (Figures 4A to 4D).

As shown in Figures 5A and 5B, neither sEHi nor ACEi treatment altered renal tissue or LV myocardial availability of biologically active epoxygenase metabolites (when expressed as the EETs/DHETEs ratio) in sham-operated HanSD rats. In ACF HanSD rats sEHi markedly increased EETs/DHETEs ratios to values observed in sham-operated HanSD rats, similarly in the kidney and in the LV myocardium. In contrast, ACEi treatment did not change EETs/DHETEs ratio values. There were no significant differences in the renal and LV myocardial 20-HETE concentrations in in any of experimental groups (data not shown).

Series 4: Effects of sEH and ACE inhibition on renal hemodynamics and excretory function

As shown in Figure 6A, untreated ACF HanSD rats showed significantly lower mean arterial pressure (MAP) as compared with untreated sham-operated HanSD rats. The treatment with either sEHi or ACEi did not change MAP in ACF HanSD rats. In contrast, treatment with ACEi significantly lowered MAP in sham-operated HanSD rats when compared with untreated and sEHi-treated sham-operated HanSD rats.

As shown in Figure 6B, there were no significant differences in the glomerular filtration rate (GFR) between any of experimental groups, however, GFR tended to be lower in ACF compared to sham-operated rats.

As shown in Figure 6C, untreated ACF HanSD rats displayed significantly lower renal blood flow (RBF) as compared with their untreated or sEHi- and ACEi-treated sham-operated

counterparts. Treatment with sEHi did not significantly change RBF in ACF HanSD rats. In contrast, ACEi treatment significantly increased RBF in ACF HanSD rats, however, it remained significantly lower than in untreated sham-operated HanSD rats.

As shown in Figures 6D and 6E, untreated ACF HanSD rats exhibited substantially lower urine flow and fractional sodium excretion as compared with untreated or sEHi- and ACEi-treated sham-operated HanSD rats. Treatment with sEHi did not increase urine flow or fractional sodium excretion in ACF HanSD rats. In contrast, treatment with ACEi raised urine flow in ACF HanSD rats to levels observed in untreated sham-operated HanSD rats and significantly increased fractional sodium excretion which, however, was still lower than in untreated sham-operated HanSD rats. Absolute sodium excretion showed a pattern similar as that seen with fractional sodium excretion (data not shown).

As shown in Figure 6F, untreated ACF HanSD rats showed markedly higher fractional potassium excretion than was observed in untreated or sEHi- or ACEi-treated sham-operated HanSD rats, likely due to secondary hyperaldosteronism. Treatment with sEHi did not alter fractional potassium excretion in ACF HanSD rats, whereas ACEi treatment normalized fractional potassium excretion to levels observed in untreated sham-operated HanSD rats.

Series 5: Effects of sEH and ACE inhibition on basal cardiac function assessed by echocardiography and by pressure-volume analysis

Figures 7 and 8 summarize the evaluation of cardiac function by echocardiography.

As shown in Figures 7A, 7B and 7C, untreated ACF HanSD rats exhibited cardiac hypertrophy reflected by increased heart weight (HW) to BW ratio, increased cardiac output (dependent on the presence of shunt) and a significant decrease in LV fractional shortening as compared with untreated sham-operated HanSD rats, which indicated LV systolic dysfunction. Treatment with either sEHi or ACEi did not change any of these parameters, similarly in sham-operated and ACF HanSD rats. ACF HanSD rats displayed significantly lower heart rate than sham-operated rats.

As shown in Figures 8A and 8B, untreated ACF HanSD rats showed marked right ventricle (RV) and LV diastolic diameters than observed in untreated ACF HanSD rats. Treatment with either sEHi or ACEi had no effect on ventricular volumes, similarly in sham-operated and ACF HanSD rats.

As shown in Figure 8C, there was no significant difference in LV posterior wall thickness between untreated ACF HanSD rats and untreated sham-operated HanSD rats. Treatment with either sEHi or ACEi did not alter LV posterior wall thickness in sham-operated rats. In contrast, both sEHi and ACEi treatments decreased LV posterior wall thickness in ACF HanSD rats. As shown in Figure 8D, untreated sham-operated HanSD rats displayed significantly higher values of interventricular septum thickness as compared with all the other groups.

Figures 9 and 10 summarize the assessment of basal cardiac function by left ventricular pressure volume analysis. As shown in Figure 9A, untreated sham-operated HanSD rats showed significantly higher LV peak pressure than untreated ACF HanSD rats. Both sEHi

and ACEi treatments significantly lowered LV peak pressure in sham-operated HanSD rats, but did not modify it in ACF HanSD rats.

As shown in Figure 9B, untreated ACF HanSD rats exhibited significantly higher LV end-diastolic volume than that seen in untreated sham-operated HanSD rats. Treatment with either sEHi or ACEi did not change LV end-diastolic volume in sham-operated or ACF HanSD rats.

As shown in Figure 9C, untreated sham-operated HanSD rats showed significantly higher maximum rates of pressure rise [$+(dP/dt)_{max}$] than untreated ACF HanSD rats. Treatment with sEHi or ACEi significantly lowered $+(dP/dt)_{max}$ in sham-operated HanSD rats, but did not change it in ACF HanSD rats.

As shown in Figure 9D, untreated sham-operated HanSD rats exhibited significantly greater maximum rates of pressure fall [$-(dP/dt)_{max}$] as compared with untreated ACF HanSD rats. Treatment with sEHi or ACEi did not alter $-(dP/dt)_{max}$ in sham-operated or ACF HanSD rats.

Figures 10A and 10B show that untreated ACF HanSD rats exhibited markedly higher LV end-diastolic pressure and stroke work than was seen in sham-operated HanSD rats. Treatment with sEHi or ACEi did not change any of these parameters, similarly in sham-operated and ACF HanSD rats.

As shown in Figures 10C, untreated ACF HanSD rats showed a markedly smaller slope of end-systolic end-systolic pressure volume relationship (end-systolic elastance, preload and afterload-independent measure of contractility) as compared with untreated sham-operated HanSD rats. Untreated ACF HanSD rats also demonstrated lower end-diastolic pressure volume relationship, indicating enhanced LV compliance (due to chamber eccentric remodeling) (Figure 10D) compared to sham HanSD rats. The treatment with sEHi or ACEi did not change any of these parameters in ACF HanSD rats.

Discussion

The first finding of the present study is that, when assessed 10 weeks after model creation, the rat ACF-induced CHF exhibits marked activation of systemic and intrarenal vasoconstrictor/sodium retaining axis of the RAS and concomitant augmentation of circulating and renal vasodilator/natriuretic axis of the RAS. However, our results also show that ACF HanSD rats display reduced intrarenal and myocardial availability of biologically active fatty acid epoxides assessed by the ratio of EETs to DHETEs. Since the renal and myocardial generation of EETs is apparently normal, as indicated by unaltered protein expression of CYP2C23, it is likely that tissue deficiency of biologically active fatty acid epoxides in ACF HanSD rats was the result of increased conversion of EETs to DHETEs; this is indicated by increased protein expression of sEH in these animals. On the other hand, our present results show that intrarenal and myocardial activity of CYP-450-dependent ω-hydroxylase pathway was not significantly changed in ACF HanSD rats as compared with sham-operated HanSD rats, as indicated by unaltered protein expression of CYP4A and 20-HETE concentration. To the best of our knowledge, ours is the first study evaluating the role

of the interplay between RAS and CYP-derived metabolites of arachidonic acid in the pathophysiology of CHF and renal dysfunction in the model of ACF-induced CHF.

The second finding of the present study is that ACF HanSD rats exhibited renal functional impairment that is characteristic for the advanced stage of CHF: a decrease in renal blood flow (RBF), urine flow, absolute and fractional sodium excretion and an increase in fractional potassium excretion. Such renal functional impairment can be mediated by activation of the vasoconstrictor axis of the RAS and by secondary hyperadosteronism (Abassi *et al.* 2011, Braam *et al.* 2014, Cohen-Segev *et al.* 2014, Ichikawa *et al.* 1984). These findings are in accordance with the hypothesis that in ACF-induced CHF the development of renal dysfunction significantly contributes to increased mortality.

The third finding of the present study is that chronic sEH inhibition with *c*-AUCB did not increase the animals' survival rate, did not attenuate the development of renal dysfunction and did not improve cardiac geometrical characteristics and systolic and diastolic function in ACF HanSD rats. This was so despite the fact that chronic treatment with *c*-AUCB resulted in normalization of the intrarenal and myocardial availability of biologically active epoxygenase metabolites, bringing them to levels observed in sham-operated HanSD rats. In addition, our results show that chronic treatment with sEHi did not significantly alter vasoconstrictor or vasodilator axes of the RAS, as assessed in circulating blood and kidney tissue of ACF HanSD rats. These data indicate that CYP-dependent epoxygenase pathway does not substantially contribute to the pathophysiology of ACF-induced CHF and, in particular, to the development of renal dysfunction in this model.

If so, what is the actual role, if any, of decreased tissue availability of EETs in ACF HanSD rats? In ANG II-dependent models of hypertension and cardiac hypertrophy, elevated ANG II led directly to an increase sEH protein expression in the kidney and heart tissue (Ai *et al.* 2007, Kopkan *et al.* 2012). Since ACF HanSD rats exhibit a marked elevation in ANG II concentrations, one can assume that increased intrarenal and myocardial sEH protein expressions with consequent decrease of tissue EETs bioavailability observed in ACF HanSD rats results from compensatory activation of the vasoconstrictor axis of the RAS. Thus, it is conceivable that decreased intrarenal and myocardial availability of EETs in ACF HanSD may simply represent changes secondary to activation of the vasoconstrictor axis of the RAS but not a primary pathophysiological mechanism responsible for the progression of CHF.

In this context, ***the fourth finding*** of the present study is that chronic treatment with ACEi dramatically improved survival rate in ACF HanSD rats to levels observed in sham-operated HanSD rats by improving renal but not cardiac structure and function. Specifically, chronic treatment of ACF HanSD rats with ACEi substantially improved RBF, increased urine flow and sodium excretion and decreased fractional potassium excretion. All these beneficial effects were not associated with any significant changes in the kidney or in the myocardial EETs bioavailability. However, these effects were accompanied by marked suppression of plasma and kidney ANG II and further augmentation of circulating and intrarenal ANG 1-7 concentrations. In this regard, of special interest is our finding that in ACF HanSD a significant attenuation of the BW gain observed throughout the experiment could be

ascribed exclusively to ACEi treatment. Remarkably, BW was in ACEi-treated ACF HanSD rats even lower than observed in sham-operated HanSD rats. We cannot offer a fully satisfactory explanation to this intriguing observation; however we assume that the reduction of BW gain might be related to the well-recognized long-lasting natriuretic actions of ACEi treatment in ACF-induced CHF (Abassi *et al.* 2011). This assumption is supported by our findings showing that treatment with ACEi significantly increased urine flow and sodium excretion. Nevertheless, our present data do not allow to define the mechanism(s) responsible for the attenuation of BW gain and future studies are needed to address this issue.

Taken together, our present findings strongly suggest that suppression of the vasoconstrictor/sodium retaining axis of the RAS in the circulation and kidney tissue combined with a further increase in the activity of the vasodilator/natriuretic axis of the RAS are the main mechanism of protective actions of ACEi treatment against CHF-related mortality and development of renal dysfunction in ACF HanSD rats. This notion is in good agreement with our recent finding that combined suppression of the ACE-ANG II-ANG II type 1 receptor (AT_1) axis and activation of ACE type 2 (ACE 2)-ANG 1-7-Mas receptor axis of the RAS in the circulation, kidney and lung tissue is the main mechanism responsible for blood pressure-lowering effects of chronic hypoxia in Ren-2 transgenic rats (Cervenka *et al.* in press.)

Twenty weeks after creation of ACF, the heart develops marked eccentric chamber remodeling, biventricular hypertrophy and an increase in stroke work: these changes represent a response to enhanced cardiac output, dependent largely on blood recirculation via the fistula. Although load-dependent measures of LV contractility, such as fractional shortening or $+(dP/dt)_{max}$, were only moderately impaired in ACF animals, the slope of end-systolic pressure volume relationship indicated a marked systolic dysfunction (Abassi *et al.* 2011, Benes *et al.* 2011, Brower *et al.* 1996, Hutchinson *et al.* 2011, Melenovsky *et al.* 2011, Melenovsky *et al.* 2012, Oliver-Dussalut *et al.* 2010, Wang *et al.* 2003) which after some time would develop toward decompensated hypertrophy and heart failure (Abassi *et al.* 2011, Benes *et al.* 2011, Brower *et al.* 1996, Melenovsky *et al.* 2012, Oliver-Dussalut *et al.* 2010, Opie et al. 2006, Wang *et al.* 2003). In this context, it is worthwhile to emphasize that even if the progression of CHF in this model was associated with marked cardiac hypertrophy, assessed as the ratio of heart weight to BW (which increased almost twofold), echocardiographic analysis revealed a concurrent decrease in LV posterior wall thickness. These findings are in agreement with previous evaluation and it is now accepted that LV remodeling in this chronic volume overload model is characterized by eccentric hypertrophy (Brower *et al.* 1996, Hutchinson *et al.* 2011, Melenovsky *et al.* 2011). Perhaps of special interest here is also our demonstration that chronic treatment with sEHi as well as with ACEi elicited significant decreases in interventricular septum thickness in sham-operated HanSD rats. The mechanism of this change is unclear and future studies are needed to address this issue.

Interestingly, ACEi treatment did not improve cardiac performance or contractility yet resulted in a marked improvement of animals' survival. This suggests that persistent renal dysfunction rather than progressing cardiac remodeling determines long-term survival in this

model of CHF. Although ACEi was reported to have an adverse effect on early LV remodeling induced by volume overload (Ryan *et al.* 2007), our data indicate that ACEi can be extremely protective in the advanced phase volume-overload (Abassi *et al.* 2011, Benes *et al.* 2011, Brower *et al.* 1996, Melenovsky *et al.* 2012, Oliver-Dussalut *et al.* 2010, Wang *et al.* 2003). Thus, chronic ACEi treatment might delay or prevent the onset of decompensation by predominantly renal mechanisms. An obvious limitation of our study is that the findings are specific for ACF model of CHF and one cannot predict the results with the model where CHF is induced by chronic pressure overload caused by transverse aortic constriction.

In conclusion, our present results show that while chronic sEH inhibition in ACF HanSD rats normalized the intrarenal and myocardial EETs availability, it did not improve the course of CHF. On the other hand, chronic ACEi treatment considerably improved the animals' survival rate and inhibited the development of renal dysfunction, and these protective actions were associated with significant suppression of the vasoconstrictor/sodium retaining axis and activation of vasodilatory/natriuretic axis of the RAS in the circulation and kidney tissue.

ACKNOWLEDGMENTS

L.Č. and V.M. equally contributed to the results of the present study and should be considered as the first authors. This study was primary supported by the grant No. NT/14012-3/2013 awarded by the Internal Grant Agency of the Ministry of Health the Czech Republic to L.Č. Z.H. is also supported by the project of the Ministry of Health of the Czech Republic for the development of research organization 00023001 (IKEM) (institutional support). The Center for Experimental Medicine (IKEM) received financial support from the European Commission within the Operational Program Prague–Competitiveness; project "CEVKOON" (#CZ.2.16/3.1.00/22126) and this study was also result of noncommercial cooperation between IKEM and OMNIMEDICS Ltd. within the project "CEVKOON". J.D.I. was supported by NIH grant DK38226. S.H.H. was supported by a fellowship from the NIEHS Supported Basic Research Program. Partial support was provided by NIEHS Grant R01 ES02710, R01 ES013933 and P42 ES013933 and by West Coast Center U24 DK097154 awarded to B.D.H. B.D.H. is a George and Judy Marcus Senior Fellow of the American Asthma Foundation. V.M. is also supported by grants No. NT14050-3/2013 and NT 14250-3/2013 awarded by the Internal Grant Agency of Health the Czech Republic and by the grant No. 15-14200S awarded by the Grant Agency of Czech Republic and by the grant MSMT-LK12052-KONTAKT II awarded by the Czech Ministry of Education.

References

ABASSI Z, GOLTSMNA I, KARRAM T, WINAVER J, HOFFMAN A. Aortocaval fistula in rat: a unique model of volume-overload congestive heart failure and cardiac hypertrophy. J Biomed Biotechnol. 2011:729497. http://dx.doi.org/10.1155/2011/729497. [PubMed: 21274403]

AI D, FU Y, GUO D, TANAKA H, WANG N, TANG C, HAMMOCK BD, SHYY JY, ZHU Y. Angiotensin II up-regulates soluble epoxide hydrolase in vascular endothelium in vitro and in vivo. Proc Natl Acad Sci USA. 2007; 104:9018–9023. [PubMed: 17495027]

BENES J, KAZDOVA L, DRAHOTA Z, HOUSTEK J, MEDRIKOVA D, KOPECKY J, KOVAROVA N, VRBACKY M, SEDMERA D, STRNAD H, KOLAR M, PETRAK J, BENADA O, SKAROUPKOVA P, CERVENKA L, MELENOVSKY V. Effect of metformin therapy on cardiac function and survival in a volume-overload model of heart failure in rats. Clin Sci. 2011; 129:29–41. [PubMed: 21275906]

BENES J Jr. MELENOVSKY V, SKAROUPKOVA P, POSPISILOVA J, PETRAK J, CERVENKA L, SEDMERA D. Myocardial morphological characteristics and proarrhytmic substrate in the rat model of heart failure due to chronic volume overload. Anat Rec. 2011; 294:102–111.

BRAAM B, JOLES JA, DANISHWAR AH, GAILLARD CA. Cardiorenal syndrome – current understanding and future perspectives. Nat Rev Nephrol. 2014; 10:48–55. [PubMed: 24247284]

BROWER GL, HENEGAR JR, JANICKI JS. Temporal evaluation of left ventricular remodeling and function in rats with chronic volume overload. Am J Physiol. 1996; 40:H2071–H2078. [PubMed: 8945927]

BURGELOVÁ M, VAŇOURKOVÁ Z, THUMOVÁ M, DVOŘÁK P, OPOČENSKÝ M, KRAMER HJ, ŽELÍZKO M, MALÝ J, BADER M, ČERVENKA L. Impairment of the angiotensin-converting enzyme 2-angiotensin-(1-7)-Mas axis contributes to the acceleration of two-kidney, one-clip Goldblatt hypertension. J Hypertens. 2009; 27:1988–2000. [PubMed: 19593210]

COHEN-SEGEV R, FRANCIS B, ABU-SALEH N, AWAD H, LAZAROVICH A, KABALA A, ARONSON D, ABASSI Z. Cardiac and renal distribution of ACE and ACE-2 in rats with heart failure. Acta Histiochem. 2014; 116:1342–1349.

ČERVENKA L, BÍBOVÁ J, HUSKOVÁ Z, VAŇOURKOVÁ Z, KRAMER HJ, HERGET J, JÍCHOVÁ Š , SADOWSKI J, HAMPL V. Combined suppression of the intrarenal and circulating vasoconstrictor renin-ACE-ANG II axis and augmentation of the vasodilator ACE2-ANG 1-7-Mas axis attenuates the systemic hypertension in Ren-2 transgenic rats exposed to chronic hypoxia. Physiol Res. in press.

DICKSTEIN K, COHEN-SOLAL A, FILIPPATOS G, McMURRAY JJ, PONIKOWSKI P, POOLE-WILSON PA, STROMBERG A, van VELDHUISEN DJ, ATAR D, HOES AW, KEREN A, MEBAZAA A, NIEMINEN M, PRIORI SG, SWEDBERG K. Committee for practice guideline (GPG). ESC guidelines for the diagnosis and treatment of acute and chronic heart failure 2008: the task force for the diagnosis and treatment of acute and chronic heart failure 2008 of the European Society of Cardiology. Eur J Heart Fail. 2008; 10:933–989. [PubMed: 18826876]

ELMARAKBY AA. Reno-protective mechanisms of epoxyeicosatrienoic acids in cardiovascular disease. Am J Physiol. 2012; 302:R321–R330.

GARCIA R, DIEBOLD S. Simple, rapid, and effective method of producing aortocaval shunts in the rat. Cardiovasc Res. 1990; 24:430–432. [PubMed: 2142618]

GIAMOUZIS G, KALEGEROPOULOS AP, BUTLER J, KARAYANNNIS G, GEORGIPOULOU VV, SKOULARIGIS J, TRIPOSKIADIS F. Epidemiology and importance of renal dysfunction in heart failure patients. Curr Heart Fail Rep. 2013; 10:411–420. [PubMed: 24097112]

HONETSCHLAGEROVÁ Z, SPORKOVÁ A, KOPKAN L, HUSKOVÁ Z, HWANG SH, HAMMOCK BD, IMIG JD, KRAMER HJ, KUJAL P, VERNEROVÁ Z, ČERTÍKOVÁ CHÁBOVÁ V, TESAŘ V, ČERVENKA L. Inhibition of soluble epoxide hydrolase improves the impaired pressure-natriuresis relationship and attenuates the development of hypertension and hypertension-associated end-organ damage in Cyp1a1-Ren-2 transgenic rats. J Hypertens. 2011; 29:1590–1601. [PubMed: 21720266]

HUSKOVÁ Z, VAŇOURKOVÁ Z, ERBANOVÁ M, THUMOVÁ M, OPOČENSKÝ M, MULLINS JJ, KRAMER HJ, BURGELOVÁ M, ČERVENKA L. Inappropriately high circulating and intrarenal angiotensin II levels during dietary salt loading exacerbate hypertension in Cyp1a1-Ren-2 transgenic rats. J Hypertens. 2010; 28:495–509. [PubMed: 19927008]

HUTCHINSON KR, GUGGILAM A, CISMOWSKI MJ, GALANTOWICS ML, WEST TA, STEWART JA Jr. ZHANG X, LORD KC, LUCCHESI PA. Temporal pattern of left ventricular structural and functional remodeling following reversal of volume overload heart failure. J Appl Physiol. 2011; 111:1778–1788. [PubMed: 21885799]

HWANG SH, TSAI HJ, LIU JY, MORISSEAU C, HAMMOCK BD. Orally bioavailable potent soluble epoxide hydrolase inhibitors. J Med Chem. 2007; 50:3825–3840. [PubMed: 17616115]

ICHIKAWA I, PFEFFER JM, FEFFER MA, HOSTETTER TH, BRENNER BM. Role of angiotensin II in the altered renal function of congestive heart failure. Circ Res. 1984; 55:669–675. [PubMed: 6091942]

IMIG JD. Epoxide and soluble epoxide hydrolase in cardiovascular physiology. Physiol Rev. 2012; 92:101–130. [PubMed: 22298653]

KATZ AM. Pathophysiology of heart failure: identifying targets for pharmacotherapy. Med Clin North Am. 2003; 87:303–316. [PubMed: 12693727]

KOPKAN L, HUSKOVÁ Z, SPORKOVÁ A, VARCABOVÁ Š , HONETSCHLAGEROVÁ Z, HWANG SH, TASI H-J, HAMMOCK BD, IMIG JD, KRAMER HJ, BURGELOVA M, VOJTÍŠKOVÁ A, KUJAL P, VERNEROVÁ Z, ČERVENKA L. Soluble epoxide hydrolase

inhibition exhibits antihypertensive actions independently of nitric oxide in mice with renovascular hypertension. Kidney Blood Press Res. 2012; 35:595–607. [PubMed: 22948718]

KUJAL P, ČERTÍKOVÁ CHÁBOVÁ V, ŠKAROUPKOVÁ P, HUSKOVÁ Z, VERNEROVÁ Z, KRAMER HJ, WALKOWSKA A, KOMPANOVSKA-JEZIERSKA E, SADOWSKI J, KITADA K, NISHIYAMA A, HWANG SH, HAMMOCK BD, IMIG JD, ČERVENKA L. Inhibition of soluble epoxide hydrolase is renoprotective in 5/6 nephrectomized Ren-2 transgenic hypertensive rats. Clin Exp Pharmacol Physiol. 2014; 41:227–237. [PubMed: 24471737]

LEAR W, RUZICKA M, LEENEN FHH. ACE inhibitors and cardiac ACE mRNA in volume overload-induced cardiac hypertrophy. Am J Physiol. 1997; 273:H641–H646. [PubMed: 9277479]

LI N, LIU J-Y, TIMOFEYEV V, QIU H, HWANG SH, TUTEJA D, LU L, YANG J, MOCHIDA H, LOW R, HAMMOCK BD, CHIAMVIMONVAT N. Beneficial effects of soluble epoxide hydrolase inhibitors in myocardial infarction model: insight gained using metabolomics approaches. J Mol Cell Cardiol. 2009; 47:835–845. [PubMed: 19716829]

MELENOVSKY V, BENES J, SKAROUPKOVA P, SEDMERA D, STRNAD H, KOLAR M, VLCEK C, PETRAK J, BENES J Jr. PAPOUSEK F, OLIYARNYK O, KAZDOVA L, CERVENKA L. Metabolic characterization of volume overload heart failure due to aorto-caval fistula in rats. Mol Cell Biochem. 2011; 354:83–96. [PubMed: 21465236]

MELENOVSKY V, SKAROUPKOVA P, BENES J, TORRESOVA V, KOPKAN L, CERVENKA L. The course of heart failure development and mortality in rats with volume overload due to aorto-caval fistula. Kidney Blood Press Res. 2012; 35:167–173. [PubMed: 22116309]

MERABET N, BELLIEN J, GLEVAREC E, NICOL L, LUCAS D, REMY-JOUET I, BOUNOURE F, DREANO Y, WECKER D, THUILEZ C, MULDER P. Soluble epoxide hydrolase inhibition improves myocardial perfusion and function in experimental heart failure. J Mol Cell Cardiol. 2012; 52:660–666. [PubMed: 22155238]

MONTI J, FISCHER J, PASKA S, HEINING M, SCHULZ H, GOSELE C, HEUSER A, FISCHER R, SCHMIDT C, SCHIRDEWAN A, GROSS V, HUMMEL O, MAATZ H, PATONE G, SAAR K, VINGRON M, WELDON SM, LINDPAINTNER K, HAMMOCK BD, ROHDE K, DIETZ R, COOK SA, SCHUNCK W-H, LUFT FC, HUBNER N. Soluble epoxide hydrolase is a susceptibility factor for heart failure in a rat model of human disease. Nat Genet. 2008; 40:529–537. [PubMed: 18443590]

NECKÁŘ J, KOPKAN L, HUSKOVÁ Z, KOLÁŘ F, PAPOUŠEK F, KRAMER HJ, HWANG SH, HAMMOCK BD, IMIG JD, MALÝ J, NETUKA I, OŠŤÁDAL B, ČERVENKA L. Inhibition of soluble epoxide hydrolase by cis-4-[4-(3-adamantan-l-ylureido)cyclohexyl-oxy]benzoic acid exhibits antihypertensive actions in transgenic rats with angiotensin II-dependent hypertension. Clin Sci. 2012; 122:513–525. [PubMed: 22324471]

OLIVER-DUSSAULT C, ASCAH A, MARCIL M, MATAS J, PICARD S, PIBAROT P, BURELLE Y, DESCHEPPER CF. Early predictors of cardiac decompensation in experimental volume overload. Mol Cell Biochem. 2010; 338:271–281. [PubMed: 20054615]

OPIE LH, COMMERFORD PJ, GERSH BJ, PFEFFER MA. Controversies in ventricular remodeling. Lancet. 2006; 367:356–367. [PubMed: 16443044]

PACHER P, NAGAYAMA T, MUKHOPADHYAY P, BÁTKAI S, KASS DA. Measurement of cardiac function using pressure-volume conductance catheter technique in mice and rats. Nat Protoc. 2008; 3:1422–1434. [PubMed: 18772869]

PETRAK J, POSPISILOVA J, SEDINOVA M, JEDELSKY P, LORKOVA L, VIT O, KOLAR M, STRNAD H, BENES J, SEDMERA D, CERVENKA L, MELENOVSKY V. Proteomic and transcriptomic analysis of heart failure to volume overload in a rat aorto-caval fistula model provides support for new therapeutical targets – monoamine oxidase A and transglutaminase 2. Proteome Sci. 2011; 9:69. http://www.proteomesci.com/content/9/1/69. [PubMed: 22078724]

PFEFFER JM, PFEFFER MA, MIRSKY I, BRAUNWALD E. Regression of left ventricular hypertrophy and prevention of left ventricular dysfunction by captopril in the spontaneously hypertensive rat. Proc Nat Acad Sic USA. 1982; 79:3310–3314.

PFEFFER MA, PFEFFER JM, STEINBERG C, FINN P. Survival after experimental myocardial infarction: beneficial effects of long-term therapy with captopril. Circulation. 1985; 72:406–412. [PubMed: 3891136]

PIERUZZI F, ABASSI ZA, KEISER HR. Expression of renin-angiotensin system components in the heart, kidneys, and lungs of rats with experimental heart failure. Circulation. 1995; 92:3105–3112. [PubMed: 7586282]

ROGER VL. Epidemiology of heart failure. Circ Res. 2013; 113:646–659. [PubMed: 23989710]

RONCO C, HAAPIO M, HOUSE AA, ANAVEKAR N, BELLOMO R. Cardiorenal syndrome. J Am Coll Cardiol. 2008; 52:1527–1539. [PubMed: 19007588]

RUZICKA M, YUAN B, HARMSEN E, LEENEN FHH. The renin-angiotensin system and volume overload-induced cardiac hypertrophy in rats: effects of angiotensin converting enzyme inhibitor versus angiotensin II receptor blocker. Circulation. 1993; 87:921–930. [PubMed: 8443912]

RYAN TD, ROTHSTEIN EC, ABAN I, TALLAJ JA, HUSAIN A, LUCCHESI PA, DELLÍTALIA LJ. Left ventricular eccentric remodeling and matrix loss are mediated by bradykinin and precede cardiomyocyte elongation in rats with volume overload. J Am Coll Cardiol. 2007; 49:811–821. [PubMed: 17306712]

SCHROTEN NF, GAILLARD CA, van VELDHUISEN DJ, SZYMANSKI MK, HILLEGE HL, de BOER RA. New roles for renin and prorenin in heart failure and cardiorenal crosstalk. Heart Fail Rev. 2012; 17:191–201. [PubMed: 21695549]

SPORKOVÁ A, KOPKAN L, VARCABOVÁ Š , HUSKOVÁ Z, HWANG SH, HAMMOCK BD, IMIG JD, KRAMER HJ, ČERVENKA L. Role of cytochrome P-450 metabolites in the regulation of renal function and blood pressure in 2-kidney, 1-clip hypertensive rats. Am J Physiol. 2011; 300:R1468–R1475.

YANG X-P, SABBAH HN, LIU Y-H, SHAROV VG, MASCHA EJ, ALWAN I, CARRETEO OA. Ventriculographic evaluation in three rat models of cardiac dysfunction. Am J Physiol. 1993; 265:H1946–H1952. [PubMed: 8285233]

WANG X, REN B, LIU S, SENTEX E, TAPPIA PS, DHALLA NS. Characterization of cardiac hypertrophy and heart failure due to volume overload in the rat. J Appl Physiol. 2003; 94:752–763. [PubMed: 12531914]

ZHANG K, WANG J, ZHANG H, CHEN J, ZOU J, ZOU Z, WANG J, HUANG H. Mechanisms of epoxyeicosatrienoic acids to improve cardiac remodeling in chronic renal failure disease. Eur J Pharmacol. 2013; 701:33–39. [PubMed: 23313758]

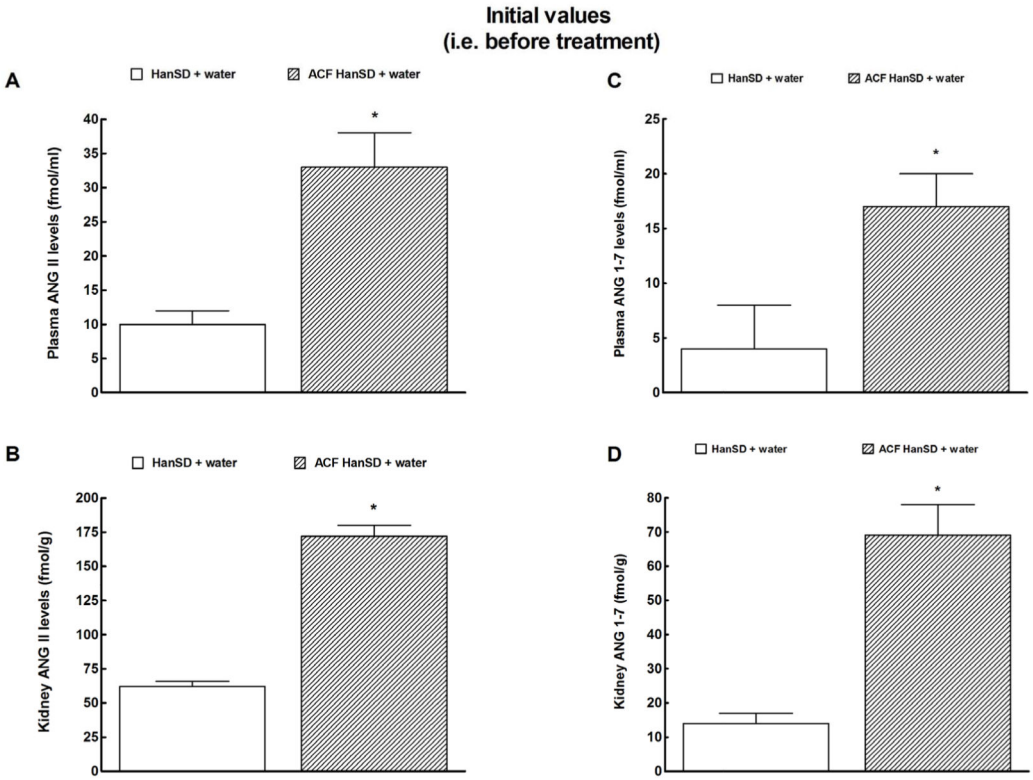

Figure 1.

Plasma angiotensin II (ANG II) (a) and angiotensin-1-7 (ANG 1-7) levels (c) and kidney ANG II (b) and ANG 1-7 (d) in untreated sham-operated Hannover Sprague-Dawley (HanSD + water) rats and in untreated HanSD rats with aorto-caval fistula (ACF HanSD + water). * $P<0.05$ compared with HanSD + water.

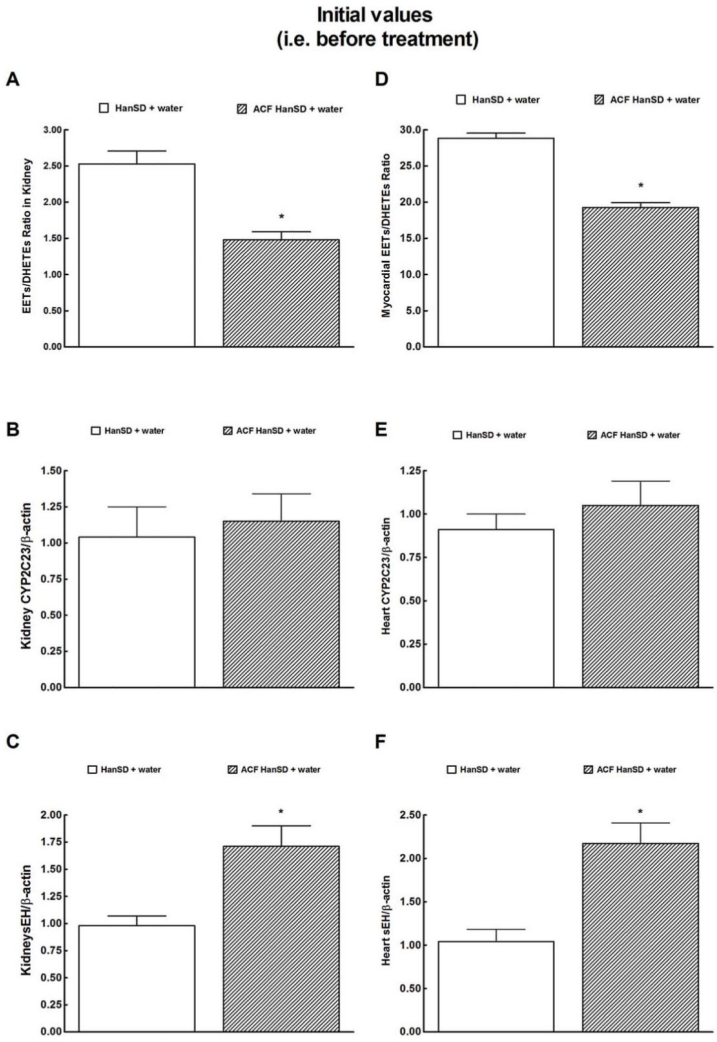

Figure 2.

Kidney and myocardial epoxyeicosatrienoic acids (EETs)/dihydroxyeicosatrienoic acids (DHETEs) ratio (a and d), expression of CYP2C23 (b and e) and soluble epoxide hydrolase (sEH) proteins (c and f) in untreated sham-operated Hannover Sprague-Dawley (HanSD + water) rats and in untreated HanSD rats with aorto-caval fistula (ACF HanSD + water). * $P<0.05$ compared with HanSD + water.

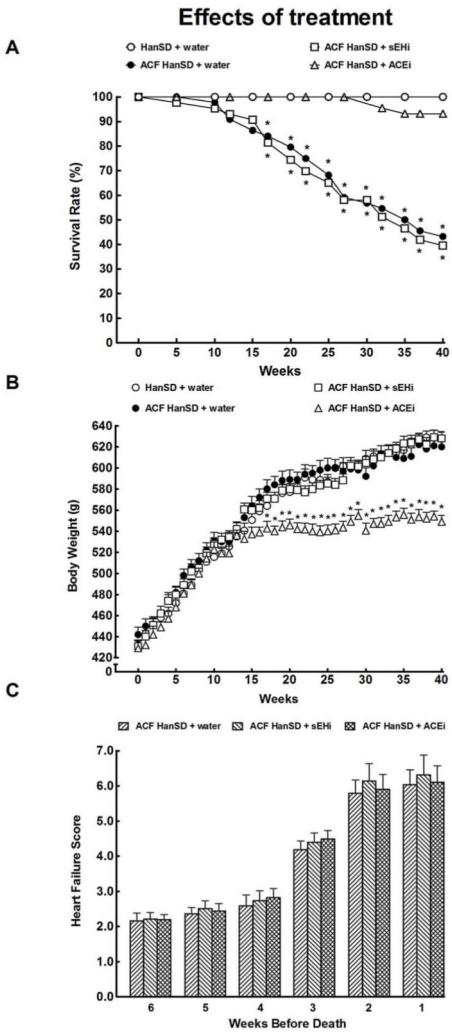

Figure 3.

Survival rates (a), body weight changes (b) and total heart failure score before death (c) in untreated sham-operated Hannover Sprague-Dawley (HanSD + water) rats, in untreated HanSD rats with aorto-caval fistula (ACF HanSD + water), in ACF HanSD rats treated with soluble epoxide hydrolase inhibitor (sEHi) (ACF HanSD + sEHi) and in ACF HanSD rats treated with angiotensin-converting enzyme inhibitor (ACEi) (ACF HanSD + ACEi). * $P<0.05$ compared with HanSD + water.

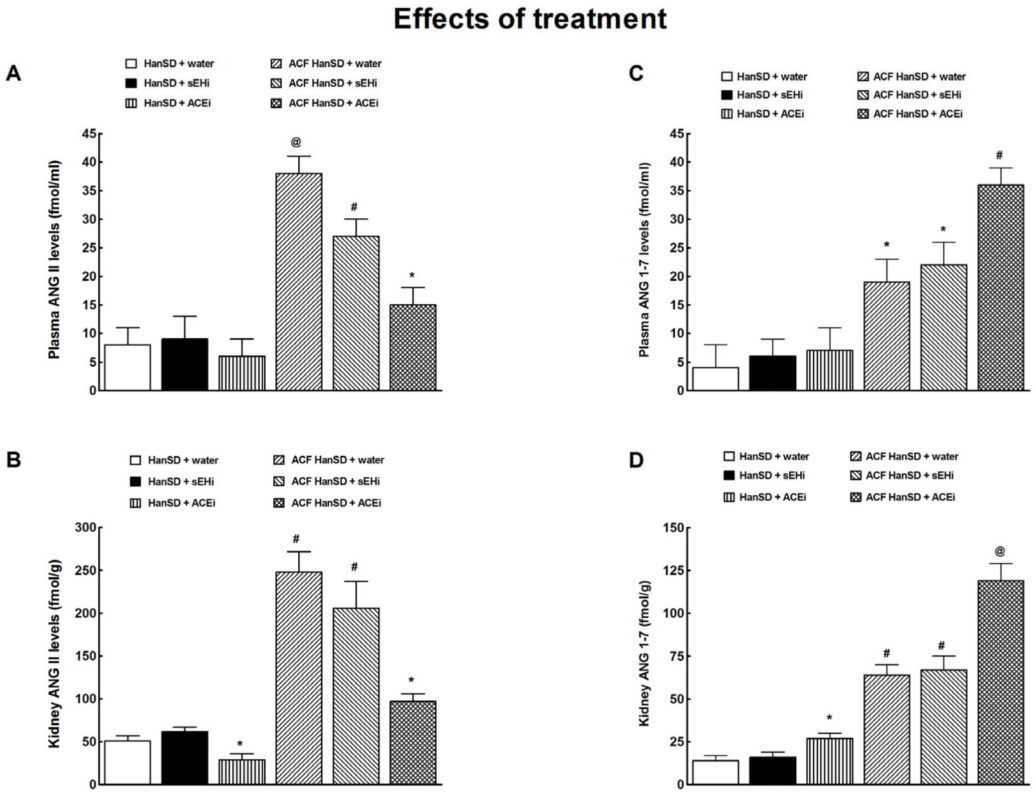

Figure 4.

Plasma angiotensin II (ANG II) (a) and angiotensin-1-7 (ANG 1-7) levels (c) and kidney ANG II (b) and ANG 1-7 (d) in untreated sham-operated Hannover Sprague-Dawley (HanSD + water) rats, in HanSD rats treated with soluble epoxide hydrolase inhibitor (sEHi) (HanSD + sEHi), in HanSD rats treated with angiotensin-converting enzyme inhibitor (ACEi) (HanSD + ACEi), in untreated HanSD rats with aorto-caval fistula (ACF HanSD + water), in ACF HanSD rats treated with sEHi (ACF HanSD + sEHi) and in ACF HanSD rats treated with ACEi (ACF HanSD + ACEi). * $P<0.05$ compared with HanSD + water. # $P<0.05$ compared with * marked values. @ $P<0.05$ compared with all other values.

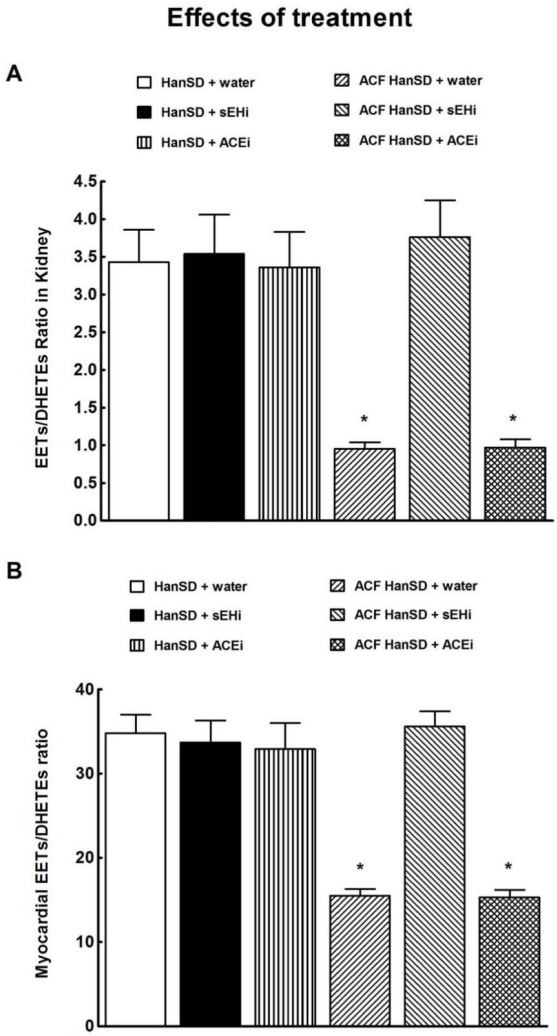

Figure 5.

Kidney (a) and myocardial (b) epoxyeicosatrienoic acids (EETs)/dihydroxyeicosatrienoic acids (DHETEs) ratio in untreated sham-operated Hannover Sprague-Dawley (HanSD + water) rats, in HanSD rats treated with soluble epoxide hydrolase inhibitor (sEHi) (HanSD + sEHi), in HanSD rats treated with angiotensin-converting enzyme inhibitor (ACEi) (HanSD + ACEi), in untreated HanSD rats with aorto-caval fistula (ACF HanSD + water), in ACF HanSD rats treated with sEHi (ACF HanSD + sEHi) and in ACF HanSD rats treated with ACEi (ACF HanSD + ACEi). * $P<0.05$ compared with HanSD + water.

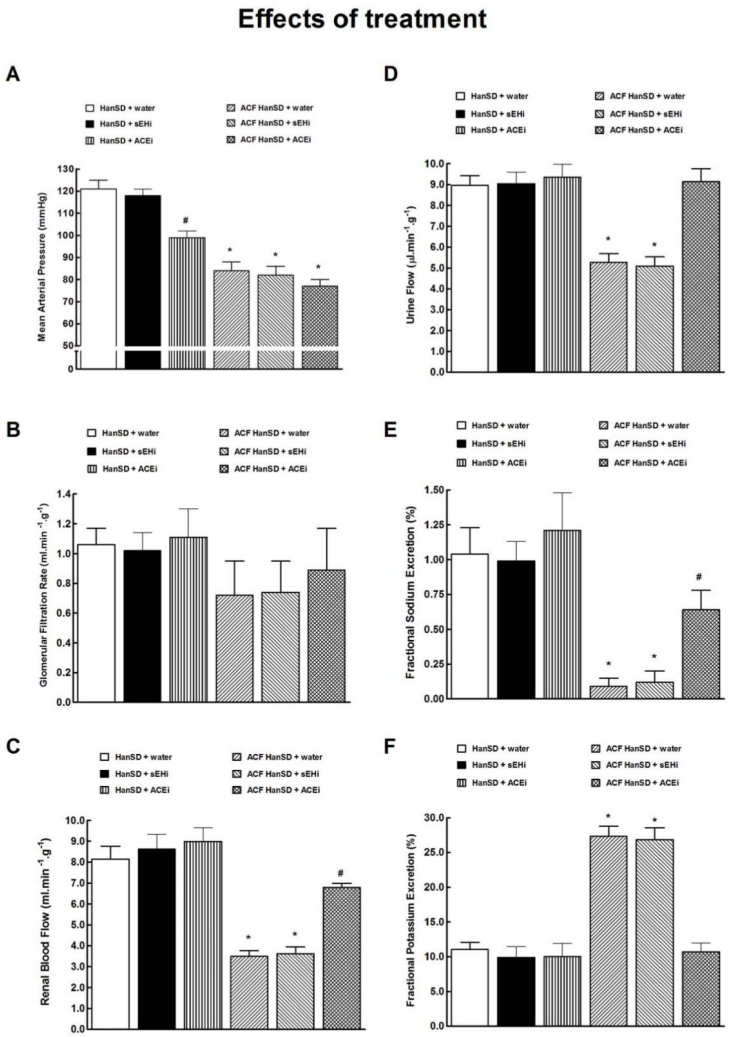

Figure 6.

Mean arterial pressure (a), glomerular filtration rate (b), renal blood flow (c), urine flow (d), fractional sodium excretion (e), fractional potassium excretion (f) in untreated sham-operated Hannover Sprague-Dawley (HanSD + water) rats, in HanSD rats treated with soluble epoxide hydrolase inhibitor (sEHi) (HanSD + sEHi), in HanSD rats treated with angiotensin-converting enzyme inhibitor (ACEi) (HanSD + ACEi), in untreated HanSD rats with aorto-caval fistula (ACF HanSD + water), in ACF HanSD rats treated with sEHi (ACF HanSD + sEHi) and in ACF HanSD rats treated with ACEi (ACF HanSD + ACEi). * $P<0.05$ compared with HanSD + water. # $P<0.05$ compared with * marked values.

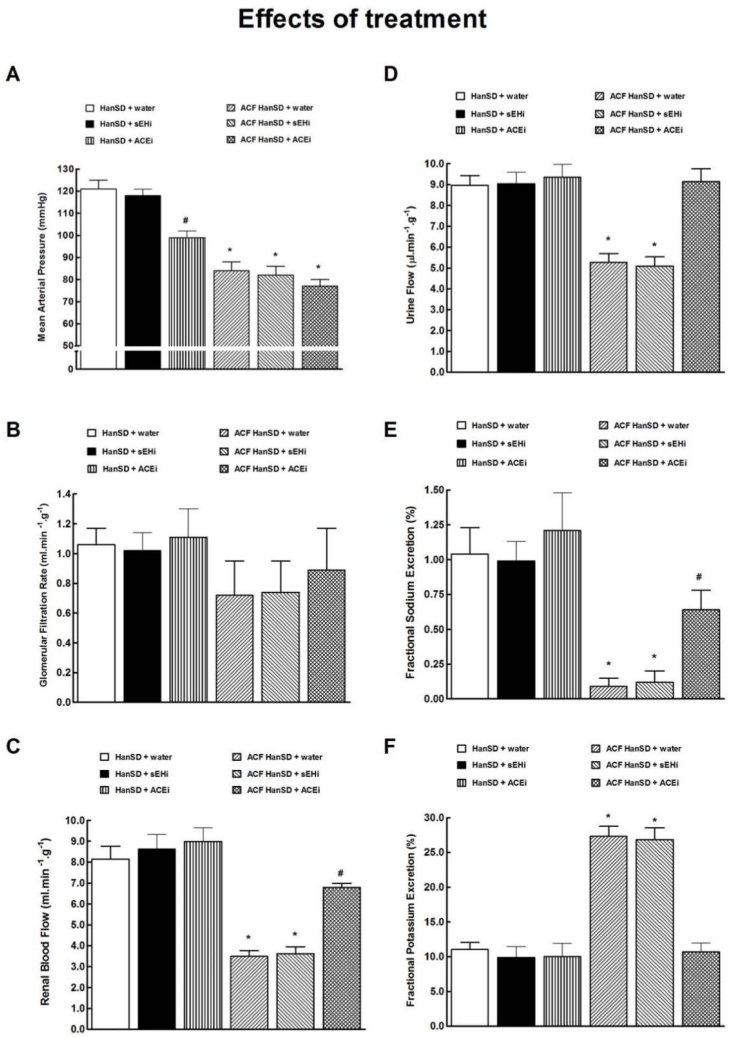

Figure 7.

Heart weight/body weight ratio (a), cardiac output (b), left ventricular fractional shortening (c) and heart rate (d) in untreated sham-operated Hannover Sprague-Dawley (HanSD + water) rats, in HanSD rats treated with soluble epoxide hydrolase inhibitor (sEHi) (HanSD + sEHi), in HanSD rats treated with angiotensin-converting enzyme inhibitor (ACEi) (HanSD + ACEi), in untreated HanSD rats with aorto-caval fistula (ACF HanSD + water), in ACF HanSD rats treated with sEHi (ACF HanSD + sEHi) and in ACF HanSD rats treated with ACEi (ACF HanSD + ACEi). * P<0.05 compared with HanSD + water.

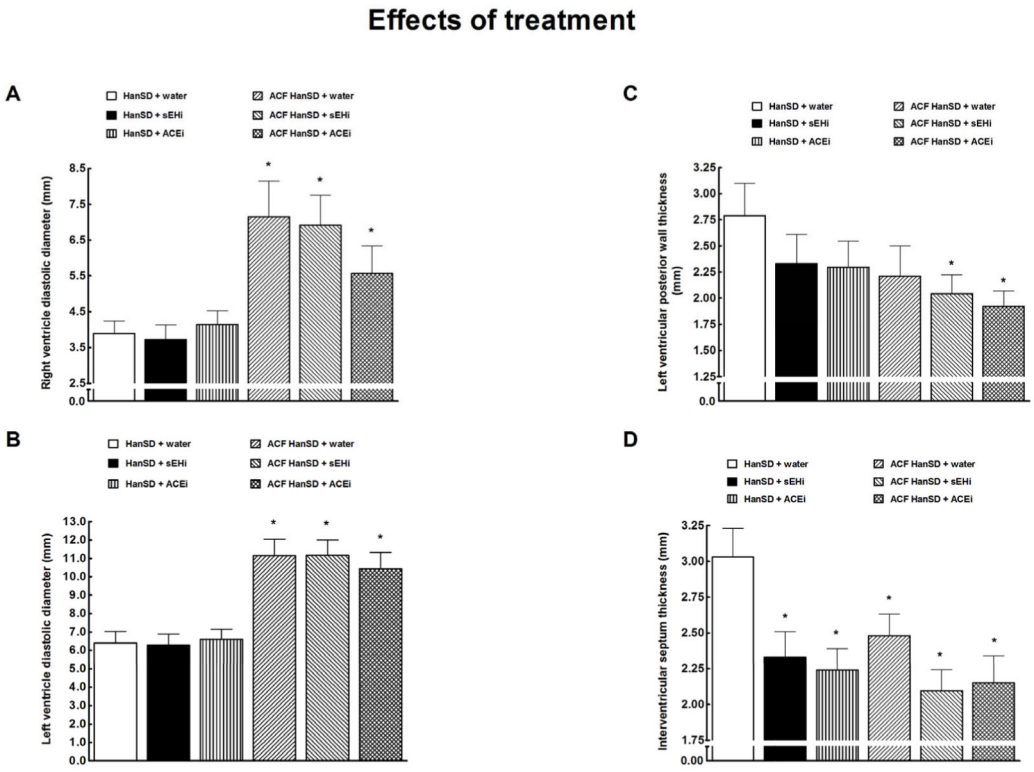

Figure 8.

Right (a) and left (b) ventricle diastolic diameter, left ventricular posterior wall thickness (c) and interventricular septum thickness (d) in untreated sham-operated Hannover Sprague-Dawley (HanSD + water) rats, in HanSD rats treated with soluble epoxide hydrolase inhibitor (sEHi) (HanSD + sEHi), in HanSD rats treated with angiotensin-converting enzyme inhibitor (ACEi) (HanSD + ACEi), in untreated HanSD rats with aorto-caval fistula (ACF HanSD + water), in ACF HanSD rats treated with sEHi (ACF HanSD + sEHi) and in ACF HanSD rats treated with ACEi (ACF HanSD + ACEi). * $P<0.05$ compared with HanSD + water.

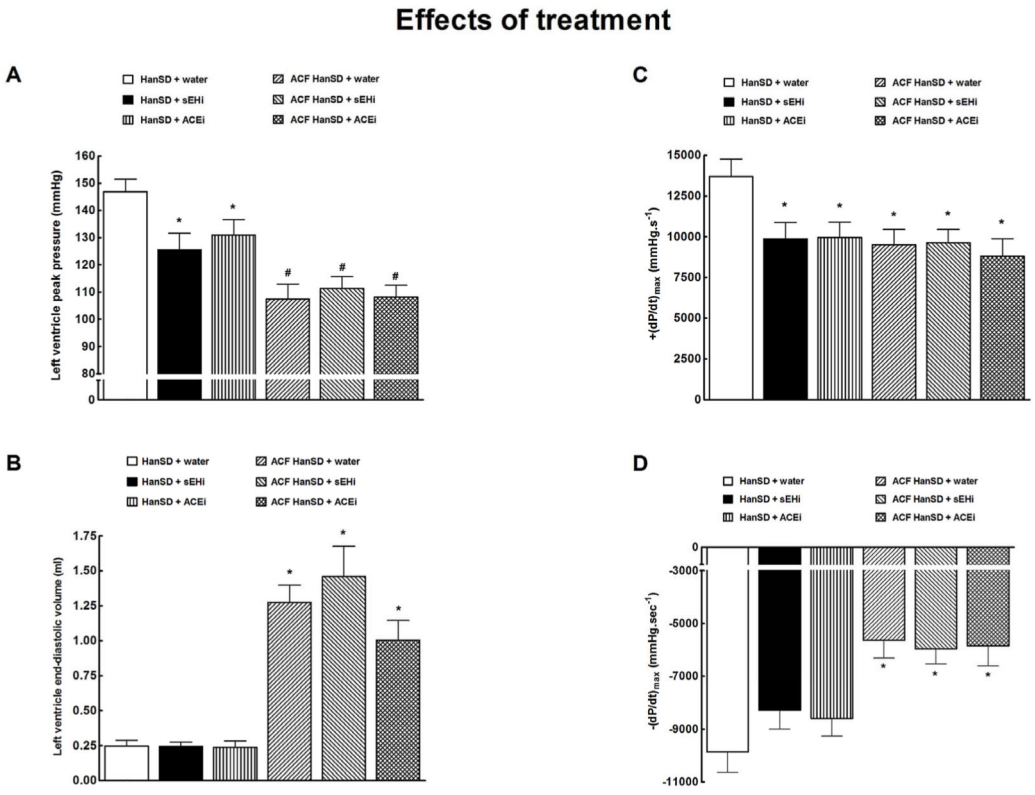

Figure 9.

Left ventricle peak pressure (a), left ventricle end-diastolic volume (b), maximum rates of pressure rise [$+(dP/dt)_{max}$] (c), maximum rates of pressure fall [$-(dP/dt)_{max}$] (d) in HanSD rats treated with soluble epoxide hydrolase inhibitor (sEHi) (HanSD + sEHi), in HanSD rats treated with angiotensin-converting enzyme inhibitor (ACEi) (HanSD + ACEi), in untreated HanSD rats with aorto-caval fistula (ACF HanSD + water), in ACF HanSD rats treated with sEHi (ACF HanSD + sEHi) and in ACF HanSD rats treated with ACEi (ACF HanSD + ACEi). * $P<0.05$ compared with HanSD + water. # $P<0.05$ compared with * marked values.

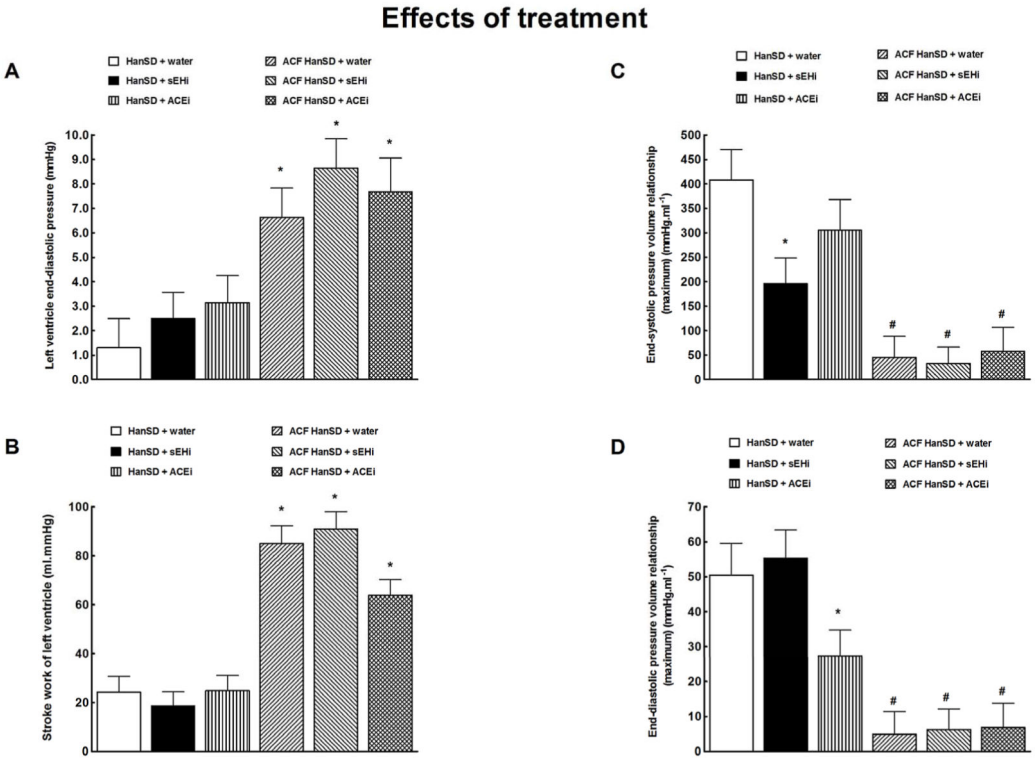

Figure 10.

Left ventricle end-diastolic pressure (a), left ventricle stroke work (b), end-systolic pressure volume relationship (c) and end-diastolic pressure volume relationship (d) in HanSD rats treated with soluble epoxide hydrolase inhibitor (sEHi) (HanSD + sEHi), in HanSD rats treated with angiotensin-converting enzyme inhibitor (ACEi) (HanSD + ACEi), in untreated HanSD rats with aorto-caval fistula (ACF HanSD + water), in ACF HanSD rats treated with sEHi (ACF HanSD + sEHi) and in ACF HanSD rats treated with ACEi (ACF HanSD + ACEi). * $P<0.05$ compared with HanSD + water. # $P<0.05$ compared with * marked values.